

# Processing of alumina-coated tetragonal zirconia materials and their response to sliding wear

S. Bueno<sup>a,b,c</sup>, B. Ferrari<sup>a</sup>, C. Melandri<sup>b</sup>, G. de Portu<sup>b</sup>, C. Baudín<sup>a,\*</sup>

<sup>a</sup> Instituto de Cerámica y Vidrio, CSIC, Kelsen 5, 28049 Madrid, Spain

<sup>b</sup> Istituto di Scienza e Tecnologia dei Materiali Ceramici, CNR, Via Granarolo 64, 48018 Faenza, Italy

<sup>c</sup> Fundación Innovarcilla - Centro Tecnológico de la Cerámica de Andalucía, Pol. Ind. El Cruce, Los Alamillos, 25, 23710 Bailén, Spain

Received 17 December 2009; received in revised form 14 January 2010; accepted 4 February 2010

Available online 9 March 2010

## Abstract

Alumina-coated tetragonal zirconia stabilised with 3 mol% of  $Y_2O_3$  (YTZP) specimens ( $30\text{ mm} \times 30\text{ mm} \times 6\text{ mm}$ ) have been obtained by dipping of pre-sintered YTZP compacts in alumina suspensions and subsequent sintering. The coated specimens present hardness values and a wear resistance similar to those of reference dense alumina specimens and significantly higher than those of the YTZP substrates.

The optimisation of the processing parameters is described. First, YTZP compacts with different open porosity levels were fabricated by colloidal filtration and subsequent thermal treatment at temperatures ranging from 1100 to 1400 °C. Coated compacts were obtained by dipping the porous ones in alumina suspensions prepared in ethanol with two different solid loadings: 3 and 10 vol.%, during immersion times up to 40 min. Sintering (1500 °C–2 h) of the coated compacts was performed and microstructural analysis allowed the selection of the optimum porosity levels for the YTZP substrates and dipping conditions. For the optimised conditions, YTZP plates ( $30\text{ mm} \times 30\text{ mm} \times 6\text{ mm}$ ) were coated and the thermal treatment to reach densification of the substrate and the coating was optimised. Relatively thick coatings ( $\cong 200\text{ }\mu\text{m}$ ) were obtained. Hardness and wear resistance were evaluated for sintered monolithic and coated YTZP compacts and an alumina reference material and the wear damage of the tested specimens was analysed.

© 2010 Elsevier Ltd and Techna Group S.r.l. All rights reserved.

**Keywords:** A. Processing; C. Wear resistance; D.  $Al_2O_3$ ; D.  $ZrO_2$ ; Coatings

## 1. Introduction

Tetragonal zirconia polycrystal doped with 3 mol% yttria (YTZP) is the monolithic ceramic that shows one of the highest combinations of fracture strength ( $>800\text{ MPa}$ ) and fracture toughness ( $5\text{--}8\text{ MPa m}^{1/2}$ ) at room temperature [1–2]. However, a widespread use of YTZP materials in some high performance structural applications is limited because of their relatively low hardness ( $H_V \cong 12\text{--}13\text{ GPa}$ ) [2] and wear resistance and the lack of stability during processes involving wet environments at temperatures in the range  $\cong 100\text{--}200\text{ }^\circ\text{C}$  as those involved the cutting of vegetables or fish or the sterilisation of YTZP hip prosthesis femoral heads [2–4]. The transformation from the metastable tetragonal

phase to the monoclinic phase under such conditions gives rise to surface degradation, increased risk of microfracture, decreased strength and, consequently, lower wear resistance [2,5–6].

Conversely, alumina materials offer a unique combination of high hardness ( $H_V \cong 18\text{--}20\text{ GPa}$ ) [2,7], corrosion resistance, thermal stability and high wear resistance [8]. The limit for the application of alumina materials is their relatively low fracture toughness ( $\cong 3\text{--}4\text{ MPa m}^{1/2}$ ) with associated low and variable strength [9].

One approach to solve the limitations of both alumina and YTZP materials is the development of monolithic composites with different proportions of alumina or zirconia as second phase, to combine the advantageous characteristics of both phases: hardness and fracture toughness, respectively. In particular, zirconia-toughened alumina (ZTA) materials with low zirconia contents as second phase ( $<15\text{ vol.}\%$ ) show higher fracture toughness than the alumina single phase while maintaining the high hardness [2,10–14].

\* Corresponding author at: Instituto de Cerámica y Vidrio, CSIC, Kelsen 5, 28049 Madrid, Spain.

E-mail address: [cbaudin@icv.csic.es](mailto:cbaudin@icv.csic.es) (C. Baudín).

However, in ZTA monolithic composites the latent possibility of transformation of the zirconia phase, possibility that continues to be extremely dependent on environmental conditions and on microstructural features determined by the manufacturing processes, is not prevented [2,10,13], even though significant microstructural advances to limit ageing have been achieved [2].

Another design strategy for improving the surface hardness of YTZP materials while avoiding the problems related to phase transformation is to produce laminated structures designed to induce compressive residual stresses at the surface by combining materials with different thermal expansions. For instance, alumina-YTZP symmetrical laminated structures in which surface alumina layers are subjected to compressive residual stresses show hardness values similar to those of monophase alumina combined with improved apparent surface fracture toughness and fracture strength [15–17]. These laminated structures have a great potential for applications involving wear processes [18].

In this work, the surface modification approach is translated into the extreme case of one single layer, i.e. coating, and the development of alumina-coated YTZP materials is proposed. It is our hypothesis that the alumina external layers would isolate the YTZP from the external environment avoiding the problems related to surface phase transformation in monolithic YTZP materials.

Efforts to obtain alumina-based coatings have been made on diverse types of substrates through different processing techniques in order to improve structural or functional properties [19–29]. As a first approach, rectangular YTZP plates were used in this work in order to characterize the wear resistance. Filtration, by dipping the YTZP plates in alumina suspensions, has been selected as the processing technique due to its relative simplicity [30]. Moreover, this shaping technique can be used to coat components with higher geometrical complexity. To achieve homogeneous microstructures a strict control of the colloidal processing was accomplished. The thermal pre-treatments of the substrates were adjusted to provide the adequate amount of open porosity to guarantee the anchoring of the coating [31] and to achieve complete densification of the coated materials avoiding extensive grain growth.

Wear tests were performed using experimental parameters that, according to our experience, can provide an extent of wear suitable for a comparison among the behaviour of the different materials tested ( $\text{Al}_2\text{O}_3$  coated YTZP, bulk YTZP, bulk  $\text{Al}_2\text{O}_3$ ) [6,11,12].

## 2. Experimental

### 2.1. YTZP compact processing and characterization

Processing of the green materials was performed by a combination of colloidal routes. Zirconia substrates were obtained by colloidal filtration of aqueous suspensions of a high purity commercial starting powder (TZ-3YS, Tosoh, Japan) following the procedure described elsewhere [32]. The

suspensions were prepared to a solid loading of 45 vol.% and ball milled with alumina jar and balls during 24 h. A commercial anionic polyelectrolyte (Dolapix CE64, Zschimmer-Schwarz, Germany) was used as dispersing aid in a proportion of 0.8 wt.% on a dry solids basis. The green compacts ( $\approx 70 \text{ mm} \times 70 \text{ mm} \times 12.5 \text{ mm}$ ) were obtained by slip casting on plaster of Paris moulds and dried in air at room temperature for at least 24 h. The apparent density of green specimens ( $\approx 10 \text{ mm} \times 10 \text{ mm} \times 10 \text{ mm}$ ) was determined by the Archimedes method using mercury.

In order to select the optimum temperature range to obtain pre-sintered YTZP substrates with different porosity levels, dynamic sintering experiments were performed on parallelepiped samples ( $6 \text{ mm} \times 4 \text{ mm} \times 4 \text{ mm}$ ) in a differential dilatometer (Adamel Lhomargy, DI24, France) up to  $1550^\circ\text{C}$  using  $5^\circ\text{C min}^{-1}$  as heating and cooling rates. One hour dwell thermal treatments at the selected temperatures ( $1100, 1150, 1250, 1300, 1350$ , and  $1400^\circ\text{C}$ ), using  $2^\circ\text{C min}^{-1}$  as heating and cooling rates, were performed in air in an electrical box furnace (Termiber, Spain). The phases present in the pre-sintered substrates were determined by X-ray diffraction (Siemens AG, D5000, Germany) and results were processed using the ASTM-Files 83–113 and 37–1484 for tetragonal and monoclinic zirconia, respectively.

The apparent density of the pre-sintered substrates was determined by the Archimedes method using mercury and water (EN 1389:2003) on samples of approximately  $10 \text{ mm} \times 10 \text{ mm} \times 10 \text{ mm}$  and the relative density was calculated using the theoretical density of  $\text{t-ZrO}_2$  ( $6.10 \text{ g/cm}^3$ , ASTM 83–113). The densities of the solid skeletons of the specimens were determined by helium pycnometry. The closed and the open porosities were calculated from these values and the theoretical density of  $\text{t-ZrO}_2$  and the apparent densities, respectively.

### 2.2. Alumina coatings processing and characterization

The alumina coatings were shaped on the YTZP compacts pre-sintered at  $1100, 1250$  and  $1300^\circ\text{C}$ . Specimens ( $10 \text{ mm} \times 7 \text{ mm} \times 7 \text{ mm}$ ) were dipped in alumina (Condea, HPA05, EE.UU) suspensions prepared in ethanol to solid loadings of 3 and 10 vol.% and using 0.5 wt.%, on a dry solids basis, of PEI (Polyethylenimine, Aldrich) as dispersant.

To obtain the alumina suspensions, the powder was added into ethanol dissolution of PEI. The suspensions were finally subjected to ultrasounds (Ultrasonication Probe, UP 400S, Hielscher, Germany) for 2 min [33]. The YTZP substrates were dipped in the alumina suspensions for immersion times up to 40 min, with a withdrawal rate of  $7 \text{ mm/s}$ . After drying in air at room temperature, the coated compacts were sintered at  $1500^\circ\text{C}$ –2 h, using  $2^\circ\text{C min}^{-1}$  as heating and cooling rates. The aspect of the sintered specimens was analysed by optical means and the polished cross sections of the pieces with apparently un-cracked coatings were observed by field emission scanning electron microscopy (FE-SEM, Hitachi, S-4700, Japan) to select the best pre-treatment and dipping conditions.

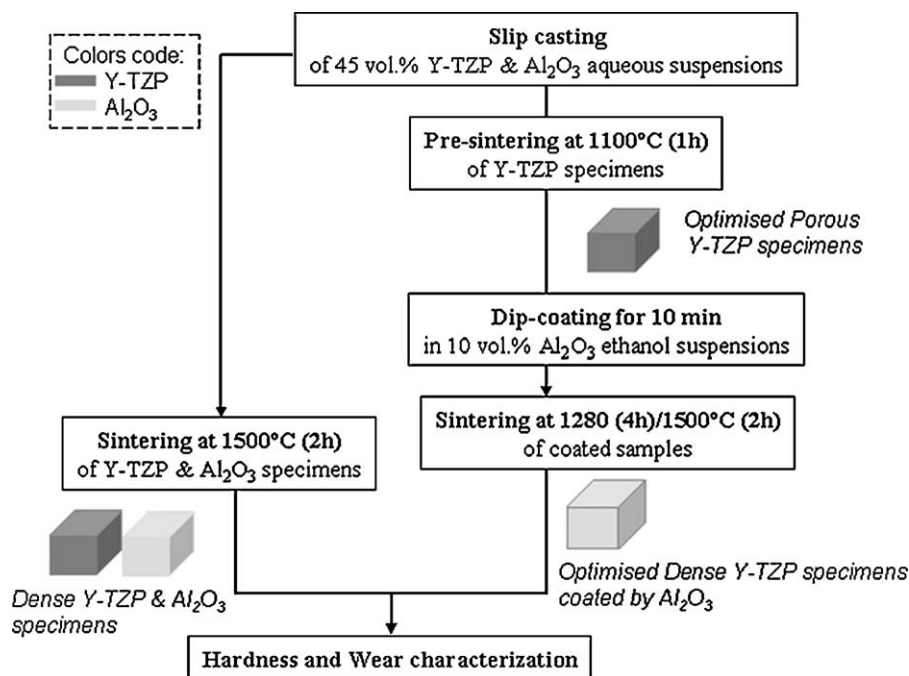


Fig. 1. Flow chart summarising the processing of the specimens used for hardness and wear.

Relatively large specimens (30 mm × 30 mm × 6 mm) for wear testing were fabricated from YTZP compacts pre-sintered at 1100 °C and dipped in the alumina suspension with 10 vol.% of solids during 10 min. In order to optimise the thermal treatment for these materials, additional dynamic sintering experiments were performed on parallelepiped samples (6 mm × 4 mm × 4 mm) of YTZP pre-sintered at 1100 °C and of an alumina compact obtained by slip casting following the procedure described elsewhere [34]. The thermal treatment selected for these relatively large wear specimens was at 1500 °C–2 h with heating and cooling rates of 2 °C min<sup>−1</sup> and 4 h dwell at 1280 °C during heating. In the next, these materials will be named AF-YTZP.

Additional specimens were fabricated from YTZP and alumina green bodies sintered at 1500 °C during 2 h.

Fig. 1 summarises the processing procedure followed to obtain the specimens used for the hardness and wear tests. Prior to testing the specimens were diamond polished down to 1 μm to reach roughness values, determined using profilometer (Taylor Hobson, Talysurf Plus, UK), of 0.02–0.03 μm.

Vickers indentation tests were performed at 10 N (Zwick, 3212, Germany) on AF-YTZP, YTZP and alumina specimens holding the load for 10 s. Optical microscopy was performed on the indented samples and hardness was calculated from the applied load and the projected areas of the residual impressions determined from the diagonal lengths.

Sliding wear tests were conducted on polished square surfaces (30 mm × 30 mm) of the AF-YTZP, YTZP and alumina specimens using an inverted pin-on-disk configuration on a tribometer (Wazau, Berlin, Germany) with unlubricated conditions. Commercial 7 wt.% cobalt-bonded tungsten carbide (WC) (ISO K20) hemispherically tipped pins were employed (diameter: 5 mm, density: 14.85 g/cm<sup>3</sup>,

hardness: 20.0 GPa). The load applied by a lever arm was 10 N, and the sliding speed 0.15 m/s. Considering the geometrical configuration and the physical–mechanical properties of the pairing materials and the applied load used it turns out an average contact stress, at the beginning of the tests, of 1.9 and 1.4 GPa for the Al<sub>2</sub>O<sub>3</sub>–WC and YTZP–WC contact, respectively. The total sliding distance was 2.5 km. The temperature and humidity of the laboratory atmosphere were kept in the range of 22 ± 1 °C and 50 ± 10%, respectively. The specific wear of the specimens was evaluated from the mass loss normalised by dividing by the applied load and the sliding distance. The depths of the wear tracks were measured in four positions, 90° apart, perpendicularly to the wear tracks, by profilometer and they were integrated using the profilometer software to obtain the wear scar area. It is well known that Al<sub>2</sub>O<sub>3</sub>–Al<sub>2</sub>O<sub>3</sub> coupling provide more severe wear conditions than Al<sub>2</sub>O<sub>3</sub>–WC because the oxidation of WC leads to the boundary lubrication case condition. However, the Al<sub>2</sub>O<sub>3</sub>–WC coupling was considered acceptable as preliminary experimental condition to compare the behaviour of the different materials studied. Moreover, a similar coupling could be present in some industrial applications.

The polished cross sections as well as the “as tested” surfaces of worn specimens were analysed by scanning electron microscopy with analysis by dispersive X-ray energy (SEM-EDX, DSM 950, Karl Zeiss, Germany).

### 3. Results and discussion

The green density of the zirconia compacts was 3.2 ± 0.1 g/cm<sup>3</sup>, which corresponded to 54% of theoretical, for a theoretical density of 6.0 g/cm<sup>3</sup>, calculated taking into account

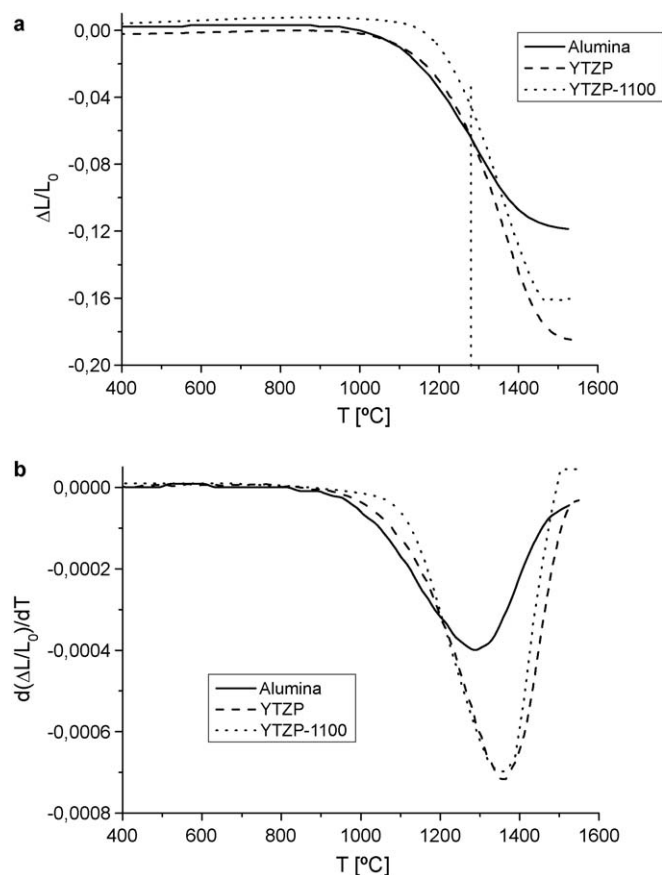


Fig. 2. Dynamic sintering curves. YTZP refers to the green compacts and YTZP-1100 to a compact pre-sintered at 1100 °C–1 h. Curves corresponding to an alumina green compact obtained by slip casting are also shown. (a)  $\Delta L/L_0$ ; linear shrinkage, versus temperature. (b) Linear shrinkage rate,  $d(\Delta L/L_0)/dT$ , versus temperature.

the phase content of the powder [33]. Fig. 2 shows the linear shrinkage curves of slip cast YTZP and alumina green compacts and of a YTZP compact pre-sintered at 1100 °C (YTZP-1100). For the YTZP green compact shrinkage starts to accelerate at approximately 1100 °C and it starts to decelerate at about 1400 °C, thus, thermal treatments inside this range were investigated for the pre-treatment of the substrates. Six isothermal thermal treatments, 1100, 1150, 1250, 1300, 1350 and 1400 °C during 1 h, were selected; tetragonal zirconia was the only crystallographic phase found by X-ray diffraction after the treatments. The values of density and porosity of the pre-

sintered compacts are collected in Table 1. The determination of apparent density by immersion in water was only possible for specimens treated at temperatures from 1250 °C due to bubble formation. In any case, values were always inside the variability limits of those determined by immersion in Hg and these latter were considered sufficiently accurate to calculate the open porosity values.

A gradual increase of the apparent density, accompanied by a significant decrease of the open porosity from 1150 to 1350 °C is observed in Table 1. Thermal treatments at 1100 and 1150 °C led to specimens with similar levels ( $\approx 40\%$ ) of open porosity and no closed porosity while the specimens sintered at 1350 and 1400 °C presented only closed porosity ( $\approx 6\%$ ). For the filtration process to occur during dipping open porosity has to be present in the substrate thus, pre-sintering treatments at 1100, 1250 and 1300 °C were selected to analyse the effect of the different open porosity levels obtained ( $\approx 40$ , 32 and 17, Table 1) on the efficiency of the dipping process.

After coating, co-sintering was performed at 1500 °C–2 h; this temperature was selected because at this temperature the reference YTZP and alumina compacts were fully dense and the use of higher temperatures could lead to undesirable YTZP and alumina grain growth.

The formation of the coating by solvent filtration into porous substrates is determined not only by the porosity degree of the substrate, but also by the solids content of the suspension and the time during which the substrate is maintained dipped. The variation of the superficial aspect of the coated specimens with the mentioned processing parameters was observed. Compacts dipped in alumina suspensions with the lowest solid loading (3 vol.%) presented similar colour and texture to those of dense YTZP materials, revealing no or extremely thin alumina coatings. When the largest solid loading (10 vol.%) was used, all coatings presented different levels of cracking except those shaped on specimens pre-sintered at 1100 °C. Apparently, these YTZP compacts with open porosities higher than 40% and ethanol suspensions with 10 vol.% of alumina led to the formation of homogeneous coatings with an adequate packing density, avoiding during sintering shrinkage gradients in the coating and/or sticking defects between the coating and the compact surface.

Consequently, further microstructural studies were performed on specimens pre-sintered at 1100 °C and dipped during 10–40 min in the alumina suspension with a solids loading of

Table 1  
Density and porosity values of the slip cast YTZP substrates pre-sintered at different temperatures.  $\rho_{Hg}$ : determined by immersion in mercury,  $\rho_{He}$ : determined by helium pycnometry,  $\rho_{H_2O}$ : determined by immersion in water. Green density of the compacts was  $3.3 \pm 0.1$  g/cm<sup>3</sup>.

| Thermal treatment | Apparent density $\rho_{Hg}$ , g/cm <sup>3</sup> | Apparent density $\rho_{H_2O}$ , g/cm <sup>3</sup> | Relative density % of theoretical | $\rho_{He}$ , g/cm <sup>3</sup> | Closed porosity, <sup>a</sup> % | Open porosity, <sup>b</sup> % |
|-------------------|--|--|-----------------------------------|---------------------------------|---------------------------------|-------------------------------|
| 1100 °C           | $3.56 \pm 0.08$                                  | –  | $58 \pm 1$                        | $6.10 \pm 0.06$                 | $\approx 0$                     | $41 \pm 2$                    |
| 1150 °C           | $3.50 \pm 0.09$                                  | –  | $57 \pm 2$                        | $6.13 \pm 0.08$                 | $\approx 0$                     | $42 \pm 1$                    |
| 1250 °C           | $4.1 \pm 0.1$                                    | $4.3 \pm 0.2$                                      | $67 \pm 2$                        | $6.08 \pm 0.05$                 | $\approx 0.3$                   | $32 \pm 1$                    |
| 1300 °C           | $5.0 \pm 0.2$                                    | $5.0 \pm 0.2$                                      | $82 \pm 3$                        | $6.05 \pm 0.07$                 | $\approx 0.8$                   | $17 \pm 2$                    |
| 1350 °C           | $5.7 \pm 0.2$                                    | $5.76 \pm 0.05$                                    | $93 \pm 3$                        | $5.74 \pm 0.06$                 | $6 \pm 1$                       | $\approx 0$                   |
| 1400 °C           | $5.6 \pm 0.1$                                    | $5.81 \pm 0.06$                                    | $92 \pm 2$                        | $5.74 \pm 0.05$                 | $6 \pm 1$                       | $\approx 0$                   |

<sup>a</sup> Calculated from  $\rho_{He}$  of the bulk specimens and the theoretical density for t-ZrO<sub>2</sub> (6.1 g/cm<sup>3</sup> from ASTM 83–113).

<sup>b</sup> Calculated from the apparent density in Hg and  $\rho_{He}$ .



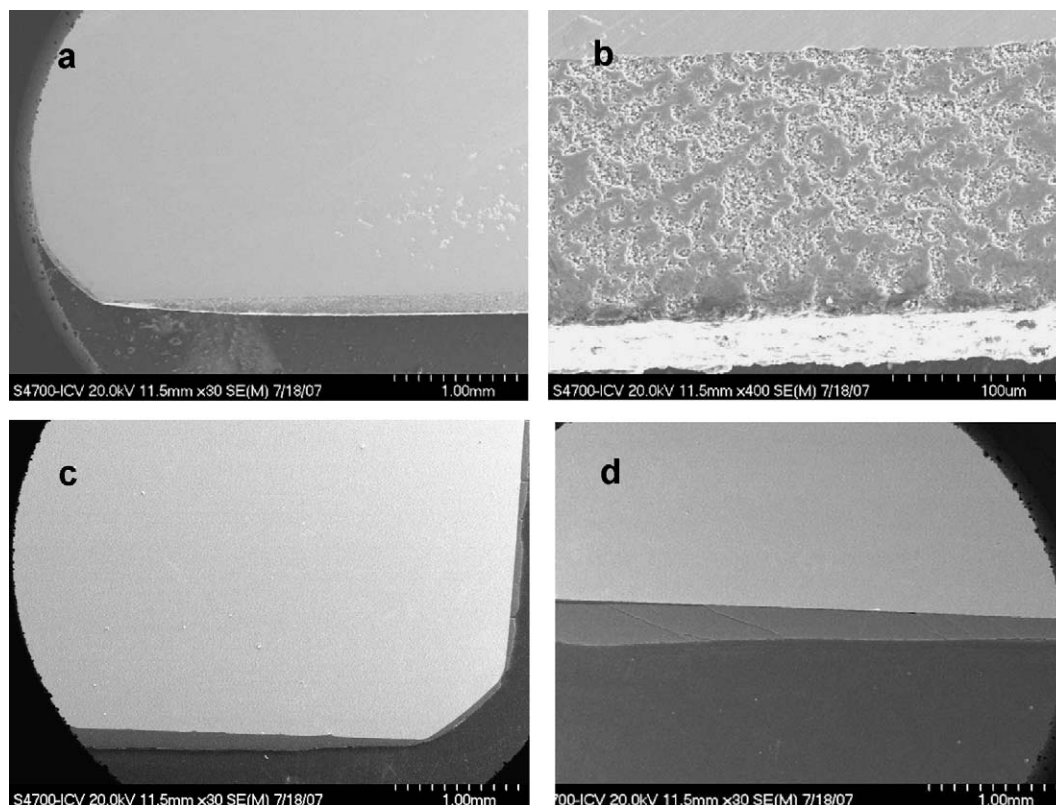


Fig. 3. Characteristic FE-SEM micrographs of the cross sections of the YTZP compacts ( $\approx 10 \text{ mm} \times 7 \text{ mm} \times 7 \text{ mm}$ ) pre-sintered at  $1100^\circ\text{C}$  and coated by dipping in an alumina suspension with a solid loading of 10 vol.%. The alumina coating (dark grey) is at the lower part of the images surrounding the YTZP compact (light grey). (a) Coating obtained by an immersion time of 10 min showing homogeneous thickness. (b) Detail of the coating obtained by an immersion time of 10 min. The presence of open porosity is detected. (c) Coating obtained by an immersion time of 20 min. Cracking of the lateral face ( $\approx 7 \text{ mm} \times 7 \text{ mm}$ ) is observed. (d) Coating obtained by an immersion time of 40 min. Cracking is also shown in the large faces ( $\approx 10 \text{ mm} \times 7 \text{ mm}$ ).

10 vol.%. In Fig. 3 characteristic cross sections of the coated and sintered specimens are shown. In general, homogeneous thicknesses between 150 and  $300 \mu\text{m}$  were obtained on the larger flat surfaces ( $\approx 10 \text{ mm} \times 7 \text{ mm}$ ) for the materials processed with immersion times from 10 to 30 min (Fig. 4a–c), whereas thicker (up to  $500 \mu\text{m}$ ) and uneven thickness was observed for the specimens dipped during 40 min (Fig. 4d). In all cases, the coating on the relatively rounded corners was thinner. Cracking of the coatings on the flat surfaces was observed for the samples dipped during more than 20 min (Fig. 4c–d). On the basis of these results, the optimum conditions to fabricate the coated specimens ( $30 \text{ mm} \times 30 \text{ mm} \times 6 \text{ mm}$ ) for hardness and sliding wear tests (AF-YTZP) were established as follows: dipping of the YTZP compacts pre-sintered at  $1100^\circ\text{C}$  in the alumina suspension with a solid loading of 10 vol.% during 10 min.

Otherwise, a closer observation of the alumina coatings (Fig. 3b) revealed significant amounts of porosity, thus, making it necessary the adjustment of the thermal treatment for sintering of the coated compacts. In Fig. 2, the dynamic sintering curve corresponding to a green alumina compact is compared to that of the YTZP substrate pre-sintered at  $1100^\circ\text{C}$ . The maximum shrinkage rate for alumina takes place at  $\approx 1280^\circ\text{C}$ , prior to the maximum rate for YTZP (Fig. 2b). At this temperature, the difference between the linear shrinkage (Fig. 2a) of alumina and YTZP-1100 materials is relatively

small ( $\Delta L/L_0 \approx 4$  and 6% for YTZP-1100 and alumina respectively). Therefore, a four hours dwell at  $1280^\circ\text{C}$  was proposed during heating in order to favour alumina densification in the coated materials.

The largest surfaces ( $\approx 30 \text{ mm} \times 30 \text{ mm}$ ) were smooth at both sides of the sintered specimens. Homogeneous coatings of about  $150 \mu\text{m}$ , with sharp and continuous interfaces between the coating and the substrate (Fig. 4a and b) were obtained, indicating that the open porosity in the pre-sintered substrates acted as efficient anchorage and that the thermal schedule was appropriate. However, partial loss of the coating occurred at the corners and lateral faces ( $\approx 30 \text{ mm} \times 6 \text{ mm}$ ), indicating that sharp corners should be avoided.

For the load value (10 N) used in the hardness tests, the sizes of the diagonals of the imprints produced in the coating were about  $33 \mu\text{m}$ , which gives a depth of  $6\text{--}7 \mu\text{m}$ , considering the Vickers indenter angle ( $136^\circ$ ), indicating that the imprints were completely embedded in the coating. Consequently, the determined hardness values of the AF-YTZP specimens ( $18.8 \pm 0.5 \mu\text{m}$ ) were similar to those of the reference alumina material ( $19.6 \pm 0.6 \mu\text{m}$ ) and significantly higher than those of the sintered YTZP compacts ( $13.4 \pm 0.4 \mu\text{m}$ ), thus, in the YTZP coated materials the relatively high hardness of the alumina materials was maintained.

The most important result related to AF-YTZP specimens refers to their behaviour under sliding wear. As shown in Fig. 5,

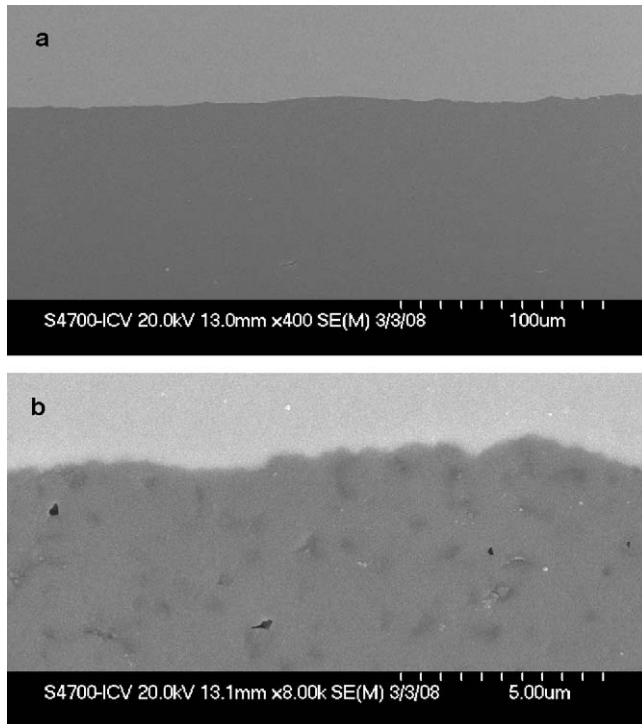


Fig. 4. Microstructure of the coated specimens (30 mm  $\times$  30 mm  $\times$  6 mm) used for the wear tests. FE-SEM micrographs of polished cross sections. The different magnifications show the sharp and continuous interfaces between the coating and the substrate and the high density and homogeneity of the coating.

the widths of the sliding tracks observed in the coatings ( $\approx 500 \mu\text{m}$ , Fig. 5b) were much smaller than those formed in the monolithic YTZP specimens ( $\approx 2500 \mu\text{m}$ , Fig. 5a) and slightly larger than those formed in the reference alumina (Fig. 5c). Moreover, the wear scar areas obtained by the profilometer software ranged from 100 to 350, 100 to 200 and 40 to 60  $\mu\text{m}^2$  for YTZP, alumina and AF-YTZP. Therefore, the depth of the wear damage in the coated specimens was much lower than that in alumina, as qualitatively observed in Fig. 6b and c.

The wear of the YTZP and alumina monoliths was similar to those previously described for similar materials [17,35].

YTZP specimens presented positive wear rate ( $2.8 \times 10^{-5} \text{ g/N km}$ ), revealing significant mass loss, and material in the wear tracks was extremely modified (Fig. 6a). The presence of  $\text{ZrO}_2$  debris plastically deformed and smeared on the specimen surface is clearly visible. No mass transfer from the pin could be detected by EDX (Fig. 6a).

On the contrary, microstructural modifications in the wear tracks of monolithic alumina and AF-YTZP were limited (Fig. 6b). Both of them presented negative wear rates ( $-5.7$  and  $-1.9 \times 10^{-6} \text{ g/N km}$  for alumina and AF-YTZP, respectively) which indicates the occurrence of mass transfer from the pin to the sample, as demonstrated by the chemical analyses (Fig. 6b).

The excellent wear resistance of the coated specimens, AF-YTZP, demonstrates the quality of the alumina coating. Moreover, as alumina has lower coefficient of thermal expansion (CTE) than zirconia, the alumina coating undergoes compressive residual stresses on cooling from the sintering

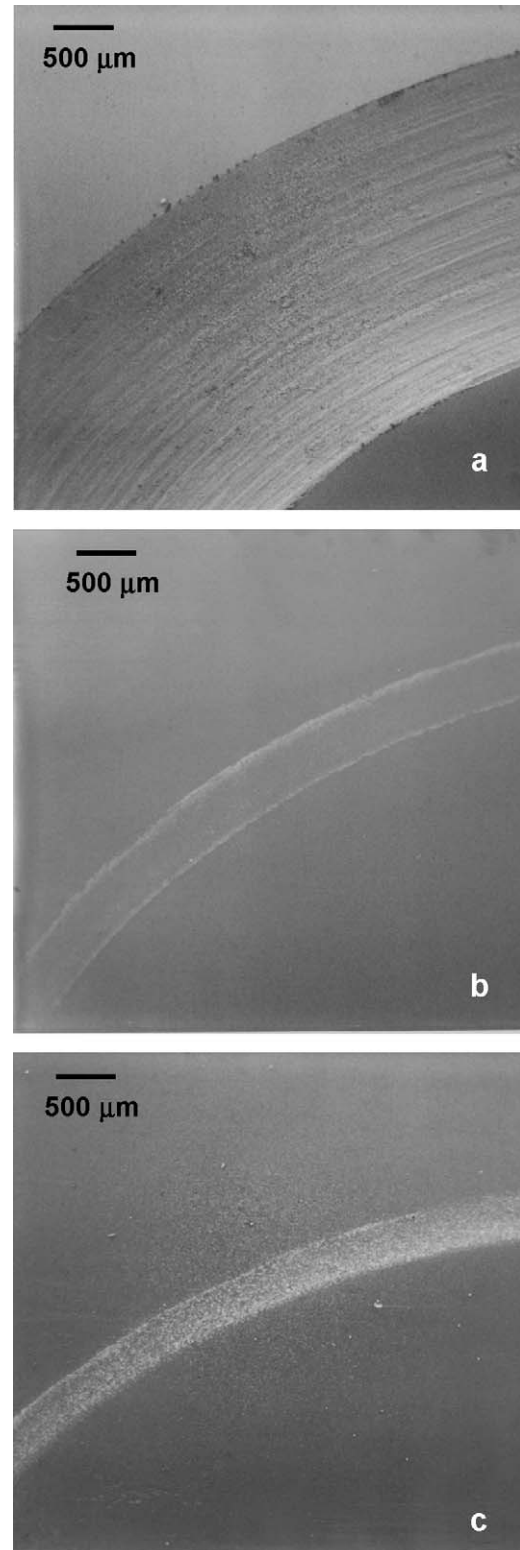


Fig. 5. Characteristic SEM micrographs showing the wear tracks in the tested specimens. (a) YTZP monolithic specimen. (b) AF-YTZP coated specimen. (c) Alumina monolithic specimen. As the magnification is the same for all the materials the different wear behaviour of YTZP appears evident.

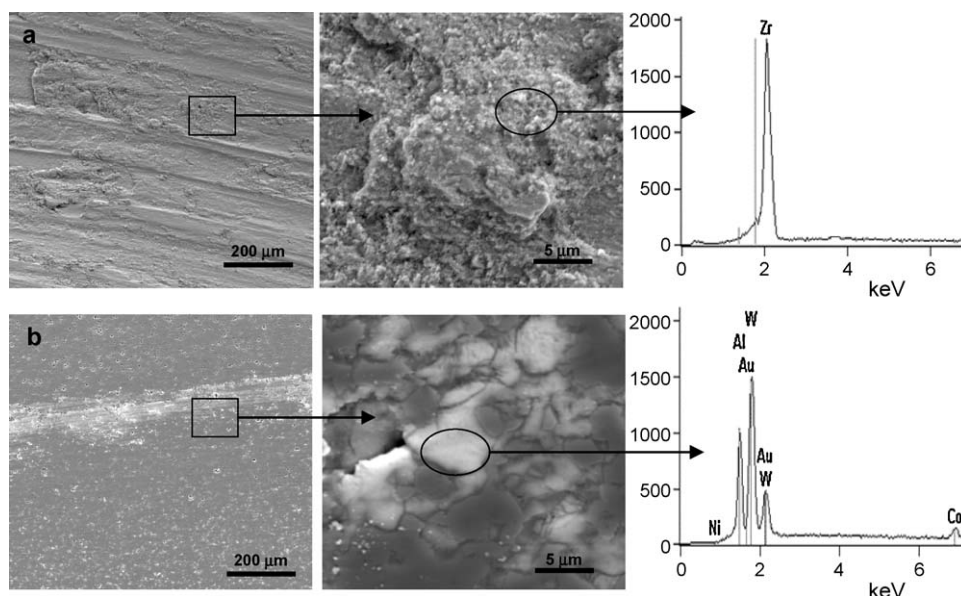


Fig. 6. Details of the wear tracks (SEM) shown in Fig. 5a and b with the corresponding EDX analysis. (a) YTZP. Extreme microstructural modifications are shown. No mass transfer from the pin is detected by EDX. (b) AF-YTZP coated specimen. Very little material modification is shown. Mass transfer from the pin is demonstrated by the presence of Co, W and Ni.

temperature. It has been demonstrated [16,36] that these stresses are beneficial in terms of wear resistance.

#### 4. Conclusions

YTZP specimens (30 mm × 30 mm × 6 mm) coated by dense and homogeneous alumina layers of about 150 μm can be obtained by dipping pre-sintered YTZP substrates with open porosities ≈40% in alumina suspensions with low solid content (10 wt.%) and subsequent sintering.

The coated specimens present hardness values similar to that of a reference dense alumina and significantly higher than that of the YTZP substrates.

The wear resistance of the coated specimens is much higher than that of monolithic YTZP. Potentially this composite could exhibit the hardness and wear resistance of alumina associated with the strength and fracture toughness of YTZP.

#### Acknowledgements

The financial support of the Project CICYT MAT2006-13480-C2 (Spain) and the Postdoctoral Fellowship MEC EX-2006-0555 (Spain) is acknowledged.

#### References

- [1] J.B. Wachtman, Mechanical properties of zirconia and zirconia-toughened alumina, in: *Mechanical Properties of Ceramics*, John Wiley & Sons, Inc., New York, 1996, pp. 391–407.
- [2] J. Chevalier, L. Gremillard, Ceramics for medical applications: a picture for the next 20 years, *J. Eur. Ceram. Soc.* 29 (7) (2009) 1245–1255.
- [3] J.L. Masonis, R.B. Bourne, M.D. Ries, R.W. McCalden, A. Salehi, D.C. Kelman, Zirconia femoral head fractures. A clinical and retrieval analysis, *J. Arthroplasty* 19 (7) (2004) 898–905.
- [4] C. Piconi, G. Maccauro, L. Pilloni, W. Burger, F. Muratori, H.G. Richter, On the fracture of a zirconia ball head, *J. Mater. Sci.: Mater. Med.* 17 (2006) 289–300.
- [5] Y. Gaillard, E. Jimenez-Pique, J.A. Munoz, J. Valle, M. Anglada, Nanoin-dentation of yttria doped zirconia under hydrothermal degradation, *Advances in bioceramics and porous ceramics*, *Ceram. Eng. Sci. Proc.* 29 (7) (2009) 77–91.
- [6] S. Conoci, C. Melandri, G. de Portu, Wear of Y-TZP containing com-pressive residual stresses at the surface, *J. Mater. Sci.* 34 (1999) 1009–1015.
- [7] S. Bueno, C. Baudin, Instrumented Vickers microindentation of alumina based materials, *J. Mater. Res.* 21 (1) (2006) 161–173.
- [8] A. Krell, D. Klaffke, Effects of grain size and humidity on fretting wear in fine-grained alumina,  $\text{Al}_2\text{O}_3/\text{TiC}$ , and zirconia, *J. Am. Ceram. Soc.* 79 (5) (1996) 1139–1146.
- [9] R.G. Munro, Evaluated material properties for a sintered  $\alpha$ -alumina, *J. Am. Ceram. Soc.* 80 (8) (1997) 1919–1928.
- [10] B. Kerkwijk, L. Winnubst, E.J. Mulder, H. Verweij, Processing of homogeneous zirconia-toughened alumina ceramics with high dry-sliding wear resistance, *J. Am. Ceram. Soc.* 82 (8) 2087–2093.
- [11] Y.J. He, A.J.A. Winnubst, D. Schipper, A.J. Burggraaf, H. Verweij, Effects of a second phase on the tribological properties of  $\text{Al}_2\text{O}_3$  and  $\text{ZrO}_2$  ceramics, *Wear* 210 (1997) 178–187.
- [12] L. Esposito, R. Moreno, A.J. Sánchez Herencia, A. Tucci, Sliding wear response of an alumina–zirconia system, *J. Eur. Ceram. Soc.* 18 (1998) 15–22.
- [13] D. Gutknecht, J. Chevalier, V. Garnier, G. Fantozzi, Key role of processing to avoid low temperature ageing in alumina zirconia composites for orthopaedic application, *J. Eur. Ceram. Soc.* 27 (2007) 1547–1552.
- [14] C. Baudín, J. Gurauskis, A.J. Sánchez-Herencia, V.M. Orera, Indentation damage and residual stress field in alumina– $\text{Y}_2\text{O}_3$ -stabilized zirconia composites, *J. Am. Ceram. Soc.* 92 (1) (2009) 152–160.
- [15] J. Gurauskis, A.J. Sánchez-Herencia, C. Baudín, Alumina–zirconia layered ceramics fabricated by stacking water processed green ceramic tapes, *J. Eur. Ceram. Soc.* 27 (2007) 1389–1394.
- [16] R. Bermejo, J. Pascual, T. Lube, R. Danzer, Optimal strength and toughness of  $\text{Al}_2\text{O}_3$ – $\text{ZrO}_2$  laminates designed with external or internal compressive layers, *J. Eur. Ceram. Soc.* 28 (8) (2008) 1575–1583.
- [17] T. Lube, J. Pascual, F. Chalvet, G. de Portu, Effective fracture toughness in  $\text{Al}_2\text{O}_3$ – $\text{Al}_2\text{O}_3/\text{ZrO}_2$  laminates, *J. Eur. Ceram. Soc.* 27 (2007) 1449–1453.

- [18] F. Toschi, C. Melandri, P. Pinasco, E. Roncari, S. Guicciardi, G. De Portu, Influence of residual stresses on the wear behaviour of alumina/alumina–zirconia laminated composites, *J. Am. Ceram. Soc.* 86 (9) (2003) 1547–1553.
- [19] K. Maca, H. Hadraba, J. Cihlar, Electrophoretic deposition of alumina and zirconia—I. Single-component systems, *Ceram. Int.* 30 (6) (2004) 843–852.
- [20] C. Kaya, F. Kaya, S. Atiq, A.R. Boccaccini, Electrophoretic deposition of ceramic coatings on ceramic composite substrates, *Br. Ceram. Trans.* 102 (3) (2003) 99–102.
- [21] S.K. Yen, S.W. Hsu, Electrolytic  $\text{Al}_2\text{O}_3$  coating on Co–Cr–Mo implant alloys of hip prosthesis, *J. Biomed. Mater. Res.* 54 (3) (2001) 412–418.
- [22] J.E. Lee, J.W. Kim, Y.G. Jung, In-situ fabrication and microstructure of alumina–zirconia layered rolling bearing in aqueous system, *Mater. Sci. Forum* 449–452 (2004) 705–708.
- [23] A.A. Abdel-Samad, A.M.M. El-Bahloul, E. Lugscheider, S.A. Rassoul, A comparative study on thermally sprayed alumina based ceramic coatings, *J. Mater. Sci.* 35 (12) (2000) 3127–3130.
- [24] O. Sarikaya, Effect of some parameters on microstructure and hardness of alumina coatings prepared by the air plasma spraying process, *Surf. Coat. Technol.* 190 (2–3) (2005) 388–393.
- [25] I. Gurappa, Development of appropriate thickness ceramic coatings on 316 L stainless steel for biomedical applications, *Surf. Coat. Technol.* 161 (1) (2002) 70–78.
- [26] G. Carta, G. Rossetto, P. Zanella, S. Battaini, S. Sitran, P. Guerriero, G. Cavinato, L. Armelao, E. Tondello, Synthesis and characterization of metal oxide multilayers obtained via MOCVD as protective coatings of graphite against oxidation, *Surf. Coat. Technol.* 160 (2–3) (2002) 124–131.
- [27] K.S. Ravichandran, K. An, R.E. Dutton, S.L. Semiatin, Thermal conductivity of plasma-sprayed monolithic and multilayer coatings of alumina and yttria-stabilized zirconia, *J. Am. Ceram. Soc.* 82 (3) (1999) 673–682.
- [28] A. Pajares, L.H. Wei, B.R. Lawn, N.P. Padture, C.C. Berndt, Mechanical characterization of plasma sprayed ceramic coatings on metal substrates by contact testing, *Mater. Sci. Eng. A—Struct. Mater. Prop. Microstruct. Process.* 208 (2) (1996) 158–165.
- [29] Y. Matsunaga, K. Mashino, Y. Shigegaki, T. Araki, N. Mori, Y. Tsuda, H. Matsubara, The high temperature oxidation behavior of CoNiCrAlY bond coating with alumina layer deposited by EB-PVD method, *J. Jpn. I. Met.* 69 (1) (2005) 80–85.
- [30] B. Ferrari, R. Moreno, Ni–YSZ graded coatings produced by dipping, *Adv. Eng. Mater.* 6 (12) (2004) 969–971.
- [31] M.G. Pontin, F.F. Lange, A.J. Sánchez-Herencia, R. Moreno, Effect of unfired tape porosity on surface film formation by dip coating, *J. Am. Ceram. Soc.* 88 (10) (2005) 2945–2948.
- [32] E. López-López, C. Baudín, R. Moreno, Thermal expansion of zirconia–zirconium titanate materials obtained by slip casting of mixtures of YTZP– $\text{TiO}_2$ , *J. Eur. Ceram. Soc.* 29 (15) (2009) 3219–3225.
- [33] B. Ferrari, A. Bartret, C. Baudín, Sandwich materials formed by thick alumina tapes and thin layered alumina–aluminium titanate structures shaped by EPD, *J. Eur. Ceram. Soc.* 29 (2009) 1083–1092.
- [34] S. Bueno, R. Moreno, C. Baudin, Design and processing of  $\text{Al}_2\text{O}_3$ – $\text{Al}_2\text{TiO}_5$  layered structures, *J. Eur. Ceram. Soc.* 25 (2005) 847–856.
- [35] S. Conoci, C. Melandri, G. de Portu, Wear of 3Y-TZP containing compressive residual stresses at the surface, *J. Mater. Sci.* 34 (1999) 1009–1015.
- [36] G. de Portu, L. Micele, D. Prandstraller, G. Palombarini, G. Pezzotti, Abrasive wear in ceramic laminated composites, *Wear* 260 (9–10) (2006) 1104–1111.